Strål säkerhets myndigheten
Swedish Radiation Safety Authority

Author: Jiaxin Chen

Research

2015:07

TEM-lamella lift-out from the crack tip region of Alloy 600 for high resolution electron microscopy examination

Report number: 2015:07 ISSN: 2000-0456
Available at www.stralsakerhetsmyndigheten.se

SSM perspective

Background
In light water reactors, various types of materials are exposed to high temperature and high pressure water environments. The impurities in reactor water may come from corrosion of various reactor materials, degradation of ion exchanger resins, or other unintended inclusions in the reactor systems. The question about how material degradation is affected by these impurities has, however, not been fully understood at present. To understand the cracking mechanism and the environmental influence, it is essential that various phenomena occurring at the crack tip can be studied. Investigation methods that enables detailed studies of the crack-tip region are therefore of highest interest.

Objectives
The objective is to develop a simple and accurate method to find crack tips and to prepare high quality TEM-lamellas which can be used to examine the crack-tip microstructure.

Summary
This report contributes to the development of a method for high-quality TEM lamella preparation from crack tip regions of nuclear materials. A standard compact tension (CT) specimen of Alloy 600 previously tested for stress corrosion crack growth in simulated PWR primary water was used to demonstrate the benefit of the proposed method. This report describes the procedure for cutting the CT specimen in order to access the crack tip region, and how TEM lamellas including crack tips were extracted with the use of Focused Ion Beam. Some high quality TEM images of crack tip regions were presented.

Sammanfattning
Föreliggande arbete syftar till utveckling av en metod för framställning av högkvalitativa tunna skivor från sprickspetsområden i nukleära material, vilka sedan kan undersökas i transmissionselektronmikrosskop (TEM). Ett standardiserat CT-prov av materialet Alloy 600 som testats i simulerad PWR-miljö i samband med spricktillväxtmätningar användes för att visa fördelarna med den föreslagna metoden. Kapning av CT-prov för att få tillgång till sprickspetsområdet och sökning efter intressanta sprickspetsar med hjälp av Focused Ion Beam (FIB) beskrivs. Några högkvalitativa TEM-bilder på sprickspetsar presenteras i rapporten.

Project information
Contact person SSM: Peter Ekström
Reference: SSM2012-4665

Strål
säkerhets
myndigheten
Swedish Radiation Safety Authority

Author: Jiaxin Chen
Studsvik Nuclear AB

2015:07

TEM-lamella lift-out from the crack tip region of Alloy 600 for high resolution electron microscopy examination

Date: August 2014
Report number: 2015:07 ISSN: 2000-0456
Available at www.stralsakerhetsmyndigheten.se

This report concerns a study which has been conducted for the Swedish Radiation Safety Authority, SSM. The conclusions and viewpoints presented in the report are those of the author/authors and do not necessarily coincide with those of the SSM.

SSM 2015:07

Content

1. Introduction

In light water reactors, various types of materials are exposed to high temperature and high pressure water environments. The impurities in reactor water may come from corrosion of various reactor materials, degradation of iron exchanger resins, or other unintended inclusions in the reactor systems. The question about how material degradation is affected by these impurities has, however, not been fully understood at present. In some power plants, zinc injection and increasing lithium levels in reactor water are introduced to minimize radiation field buildup. Moreover, an optimized hydrogen level in reactor water is also under consideration with the aim of decreasing crack growth rates of reactor nickel based alloys. Although some operating experiences with these proactive water chemistry management programs have indicated promising results, the mechanisms about how these changes in corrosion environments affect material crack growth rates remain largely to be explored.

Take the effect of hydrogen on primary water stress corrosion cracking (PWSCC) initiation and propagation for an example. This issue has been studied for Alloy 600 in simulated PWR conditions at Studsvik [1–6] and elsewhere [e.g. 7-12]. It is generally agreed that the crack growth rate reaches a maximum at about 20 cc H_2/kg H_2O dissolved hydrogen level (at 330°C) in reactor water, below or above which the crack growth rate would be decreased. See Figure 1.

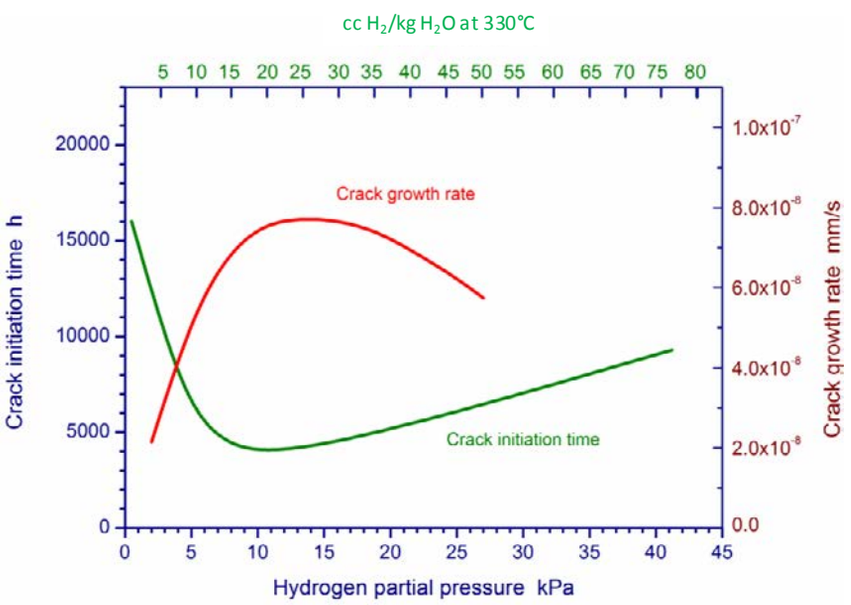

Figure 1
Comparison of CGR and initiation data versus the hydrogen content for Alloy 600 material in simulated PWR conditions. After ref (5).

In a recent study [6], the crack growth rates of a heat of Alloy 600 were again measured in simulated PWR primary water environment with two dissolved hydrogen levels; 5 and 75 cc H_2/kg H_2O, respectively. The general trend as depicted in Figure 1 was confirmed by the study. However, to understand the possible mechanisms behind the decreased crack growth rates at the low and high dissolved hydrogen levels, much more detailed information about the microstructures of the crack tip regions, such as oxide film morphology and compositions as well as defect structures, would be required than what was available at the time.

Staehle [13] considered that the relatively long crack path from the bulk water to the crack tip, and the small size of the crack tip may make the local chemical environment close to the crack tip drastically different from bulk water chemical environment. The width of a stress corrosion crack (SCC) may be as small as 1 nm. He compared this space with an equivalent size of e.g. three water molecules, three metal atoms, two sulfate ions, two electrical double layers and two bi-atomic layer passive films; see Figure 2. At the crack tip, the energy barrier for a chemical reaction to occur could be very different due to possibly significant contribution of surface energy of the fresh cracking surface. In such an environment, our previous knowledge that was derived from observations of material-water interaction in bulk water environments may not always be valid. To understand the cracking mechanism and environmental influence, it is essential that various phenomena occurring at the crack tip are known.

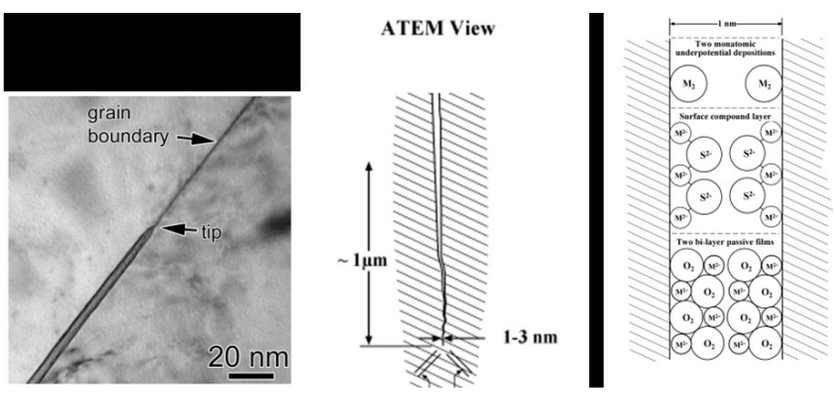

Figure 2
Crack tip view and its dimension compared to that of possibly involved chemical species. After ref. [13].

Analytical transmission electron microscopy (ATEM) was early on adopted for studying crack tip microstructure [e.g. 12], and some interesting observations have been made for Alloy 600. In these studies, cross-sectioned TEM lamellas were prepared by conventional TEM sample preparation techniques including cutting, grinding, polishing, dimple-grinding and finally ion milling. Since the crack tip is small and possibly reactive, it is anticipated that any unwanted chemical reactions during the sample preparation would result in misleading results.

In recent years, Focused Ion Beam (FIB) has been widely applied to prepare high quality TEM lamellas. Compared to the conventional TEM sample preparation technique mentioned above, FIB has the following advantages of great significance:

- One can precisely choose a micro-area which includes a crack tip to prepare a high quality TEM-lamella. With the conventional methods mentioned above, this would be difficult;
- One may do TEM-lamella thinning at some selected regions of interest with FIB/SEM with well-controlled energy of the incident Ga^+ ion beam so that the Ga^+ ion beam induced artifacts could be effectively minimized; With the conventional methods, this would be more difficult to achieve;
- One can prepare a TEM-lamella in high vacuum system of FIB/SEM and then quickly transfer the lamella to the high vacuum system of TEM. This would minimize possible reactions between the fresh TEM-lamella and the ambient environment. With the conventional methods, there is a high probability that during the TEM-lamella preparation the crack tip is exposed to corrosive environments which may introduce unspecified artifacts.

Application of FIB for nuclear material examination has got some momentum in recent years due to its obvious advantages In fact, the use of FIB to prepare TEM-lamella for crack tip examination has already started to appear in open literature, although the details about sample preparation are rare. In a most recent paper [15], however, the common chemical etching and electro-jet polishing were still used in sample preparation before a TEM-lamella was lifted out from a crack tip.

In this work, we have developed a new method for preparation of TEM-lamellas directly from crack tips without the above-mentioned steps of chemical etching and electro-jet polishing. The objective has been to find an easy and accurate way to find crack tips and to prepare high quality TEM-lamellas. A standard compact tension specimen that had been tested for crack growth in simulated PWR primary water environment was used in this work.

2. Experimental

2.1. Material and specimen with crack tips [6]

The test material was a 38.1 mm thick plate of Alloy 600, delivered in the mill annealed condition. Some material property data are shown in Appendix A.

A standard compact tension specimen with a thickness of 25 mm (1TCT) was prepared from the material. The specimen was oriented in the L-T direction according to ASTM E399, and it was cut so that it was centered in the thickness of the plate. Machining was performed by Electro Discharge Machining (EDM). Following machining, a dimensional check verified that all measures were within the tolerances. A schematic drawing of the specimen is shown in Figure 3.

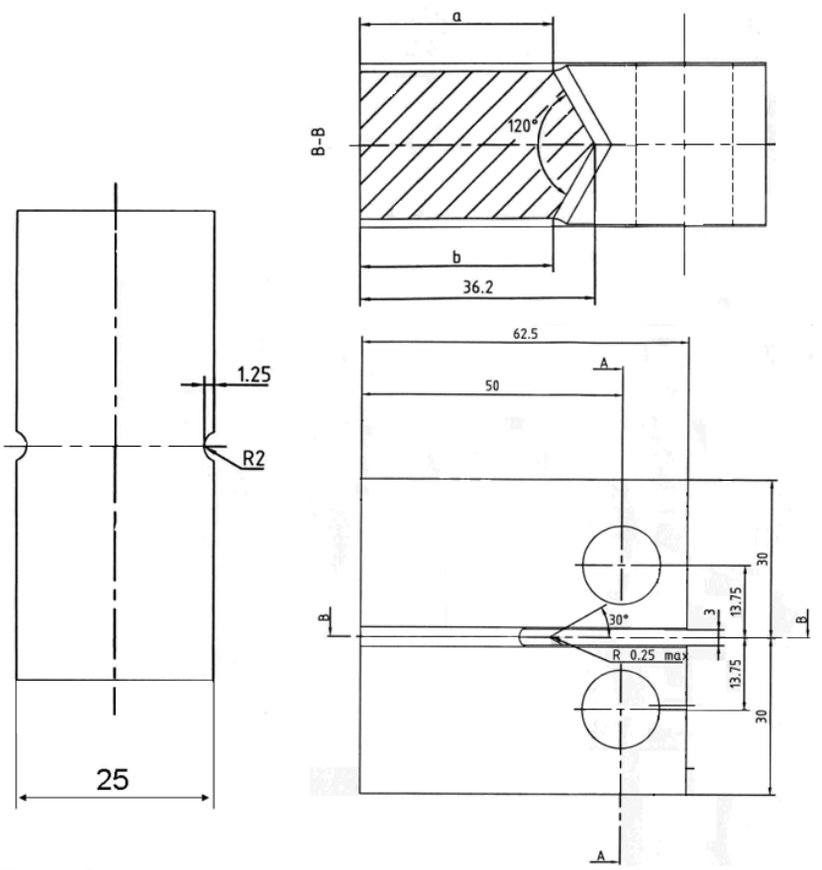

Figure 3
Schematic drawing of the 1TCT specimen used for testing (dimensions in mm).

Fatigue pre-cracking of the specimens was performed at Studsvik in room temperature air to a crack length of 25 mm (a/W=0.50). Subsequent to fatigue pre-cracking, the crack length was checked visually on the specimen's side surfaces to ensure a fairly straight crack front and a crack length close to the desired value.

The test system used was of the once-through type with a free autoclave volume of 7 liters. A schematic of the system is shown in Figure 4. Following fatigue pre-cracking, the specimen was ultrasonically cleaned in acetone and later in ethanol. The specimen was then mounted in the autoclave. The autoclave was then closed and simulated PWR-environment was gradually established. When the desired testing conditions (pressure, temperature, and water chemistry) were reached, the crack growth test started with Step 1 according to Table 1. For each step the stress intensity (K), R-ratio (defines the load amplitude), frequency of cycling (f) and crack increment was pre-defined.

Table 1
Testing procedure.

Step	K (MPa√m)	R-ratio	f (Hz)	Increment[1)] (mm)
1	25	0,3	1	0,5
2	27.5	0,5	1	0,3
3	30	0,6	1	0,3
4	30	0,7	1	0,3
5	30	0,7	0,1	0,2
6	30	0,7	0,01	0,2
7	30	0,7	0,001	0,2
8	30	0,7	0,001(9 ks hold time)	0,1
9	30	1	-	>0,1

1) According to the DCPD response.

Degassed high-purity water from the Studsvik water purification plant was fed to the autoclave system with a flow rate of ~6 liters/h through a heat exchanger and a preheater. A concentrated solution of B and Li (deaerated by bubbling N_2 gas was added to the main flow before the high-pressure pump so that it was diluted about 6 times. Inlet and outlet solution conductivities were monitored continuously with a Thornton 200CR instrument and sensors. The outlet hydrogen concentration was monitored by an Orbisphere instrument (3680/81 Multisensor Gas Analyzer). The concentrations of B, Li, chloride and sulfate of the loop water were analyzed on grab samples on a weekly basis.

Loading of the CT-specimen was controlled by an Instron Model servo electric testing machine with Model 8800 control electronics. A PC-based control and data acquisition system (based on LabView from National Instruments) was used to control the specimen load and to collect data from

the various measurements. A direct current potential drop (DCPD) system was used to monitor crack growth. The specimen was electrically isolated from the clevises and the autoclave by bushings and washers of yttria-stabilized zirconia. The data acquisition system recorded data such as crack length, specimen load, autoclave temperature, pressure, solution conductivity, and dissolved hydrogen level from the measurements. To transition the transgranular pre-crack to intergranular primary water stress corrosion cracking (PWSCC) crack, the test started with steps under cyclic load, followed by steps with gradually less aggressive loading condition (Steps 1-8 in Table 1). K_{max} during the test was 30 MPa√m. With such a procedure intergranular cracking in this material could be generated [16–18].

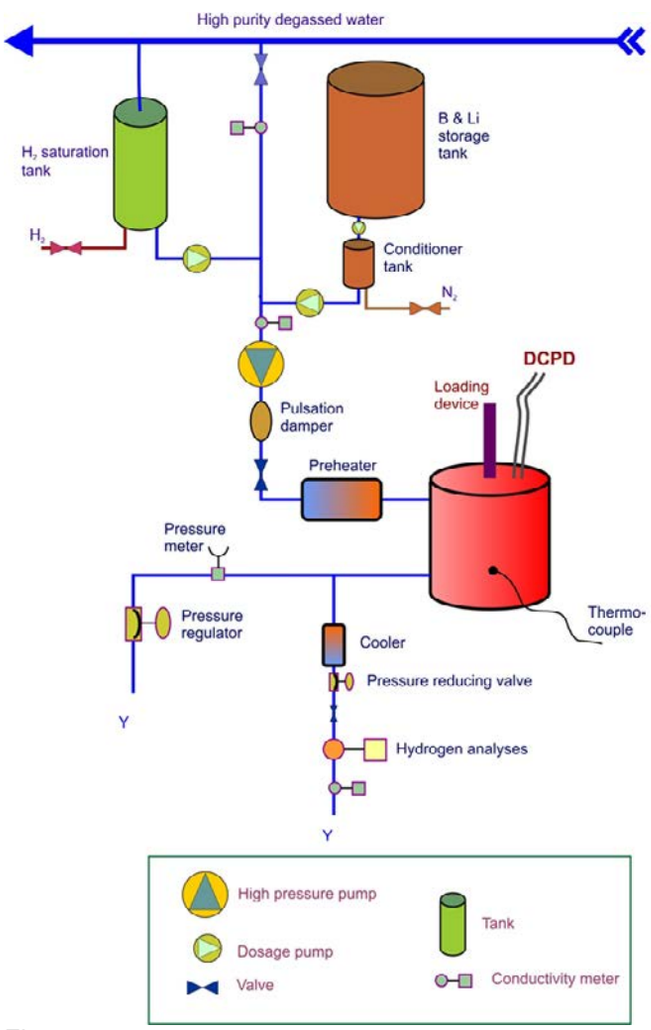

Figure 4
Flow chart of the test system.

The simulated PWR primary water contained 1200 ppm B and 2.2 ppm Li and a dissolved hydrogen level of 5 cc H_2/kg H_2O. Hydrogen was added from a saturation tank to the main flow before the high-pressure pump. The

temperature was nominally 330 ºC during the test. The quality of the water chemistry was verified by grab samples and the outlet conductivity.

After testing, the system was cooled down. The specimen load (final load or somewhat beneath, 25–30 MPa√m) was maintained during cool down of the system, and then kept by inserting a wedge at the front face of the specimen. The CT specimen was then removed from the autoclave and embedded in epoxy (EpoFix Resin, Struers) under vacuum. Finally the specimen was cut into two halves with a diamond cutting wheel. One half was broken open by fatigue in air at room temperature for fractographic examination. The other half was further cut with EDM as illustrated in Figure 5. In this process crack growth data were used to estimate the location of the crack tip. Cutting was made at a distance of a few millimeters ahead of the crack tip front. The sample was then further cut into an even smaller specimen which contained the crack tips (see the red rectangular cube in Figure 5a.

In order to reveal part of the crack, the rectangular cube was further cut at an angle of 10° as illustrated in Figure 5b and Figure 5c. Following the EDM cutting, the cut surface (Figure 5c) was ground and polished with SiC papers of various grades down to 4000 grit. Figure 6 shows the crack path observed on the cut surface. TEM-lamellas were to be lifted out in such a crack tip region.

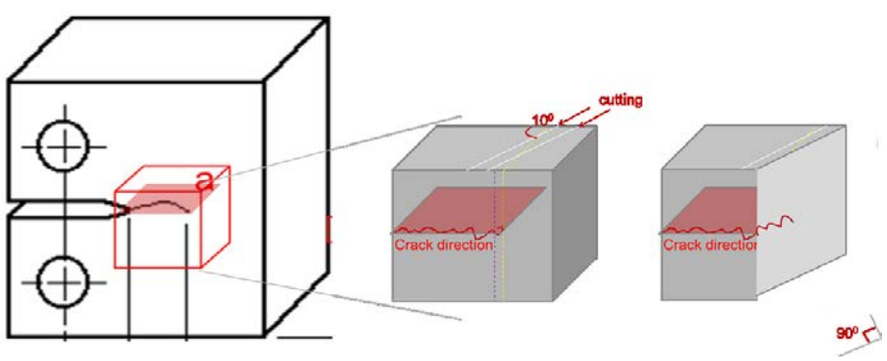

Figure 5
Schematic drawing of EDM cutting steps to obtain a piece of material including crack tips.

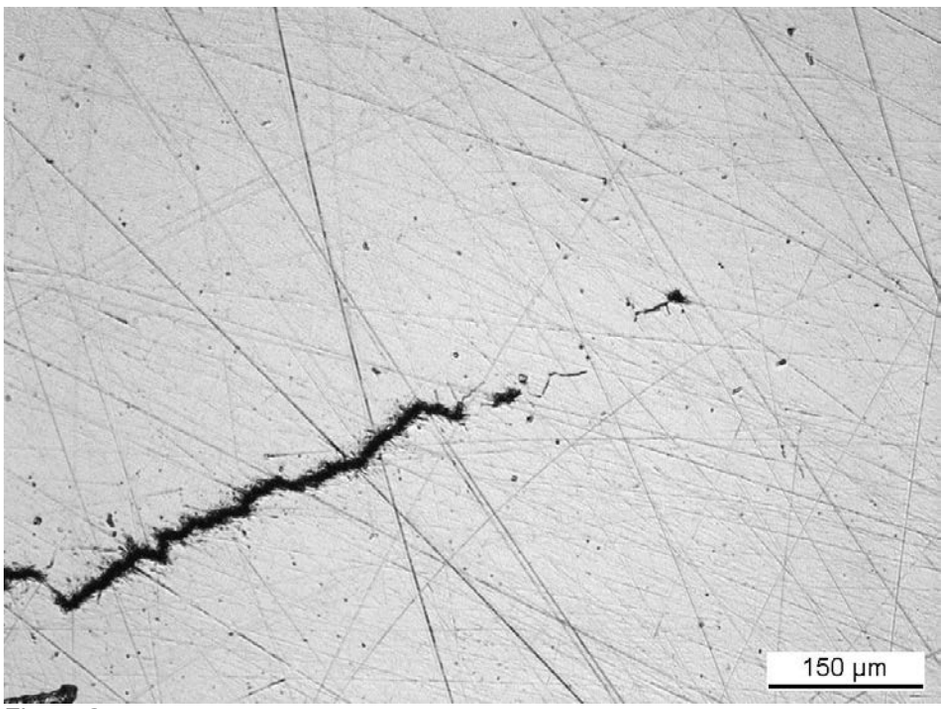

Figure 6
A stereo optical microscopy image showing the crack path in the crack tip region.

After one TEM-lamella was prepared, the surface was ground and polished to reveal a new surface containing the crack tip; see schematic illustration in Figure 7. The grinding depth was estimated by measuring the sample weight before and after grinding and polishing.

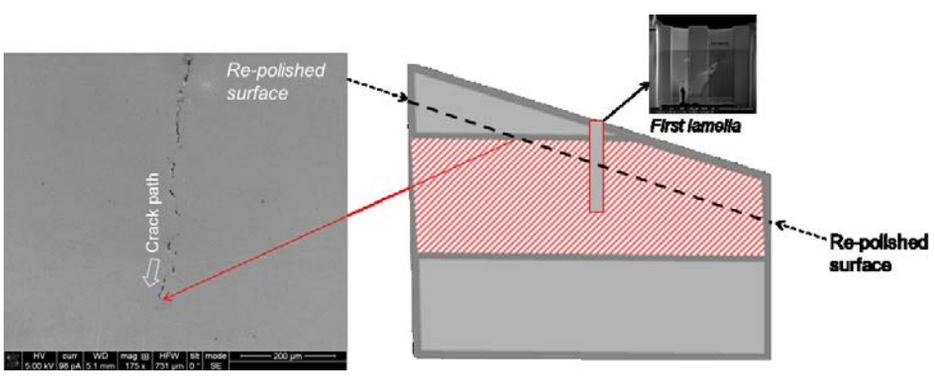

Figure 7
A schematic drawing showing a new crack tip region (arrowed) after grinding and polishing the sample surface from which the first TEM-lamella was prepared.

2.2. FIB/SEM instrumentation

A Dual-Beam system of the Nova 600 NanoLab was used to prepare TEM-lamellas from the crack tip region of the sample. The system, combining a high resolution FEG-SEM with FIB, was used to search for and to accurately identify the locations of crack tips on the above-mentioned sample surfaces. To protect the metal surface from Ga^+ ion beam damage, two protective Pt layers were deposited on the metal surface, first using an Electron Beam Induced Deposition (EBID) followed by an Ion Beam Induced Deposition (IBID) of Pt. The thinning of a lamella was made progressively until its thickness became approx. 50 nm or thinner. To make a crack tip region even thinner, spot ion milling was applied. The final low-energy polishing step was performed at ion acceleration voltage and current of 5 kV and 70 pA, respectively. FIB was also used to remove material from the surface in order to reveal some cracks that were hidden under the metal surfaces. In such a case, Ga^+ ion milling was made directly on the suspected crack tip region.

2.3. TEM instrumentation

A JEOL model JEM-2100F field emission type transmission electron microscope operated at 200 kV, equipped with Energy-Dispersive X-Ray Spectroscopy (EDX) and Electron Energy Loss Spectroscopy (EELS) detectors, was used to examine the TEM-lamellas prepared from the crack tip regions. The microscope is equipped with both bright field and dark field Scanning Transmission Electron Microscopy (STEM) detectors. EDX and EELS were used, where appropriate, to determine local elemental compositions. Electron diffraction was also used to determine the crystal structure at locations of interest.

3. Results

3.1. Preparation of TEM-lamella no. 1

In Figure 8 six SEM images are shown. Figure 8a shows the location (yellow marked) for the lift-out of a TEM-lamella. The deposited Pt has the shape of a bar with a width of about 2 µm. One side of the bar-shaped Pt deposit was very close to the crack tip. Two large cracks appeared (Figure 8b) once the material in this area was removed with the FIB. On the other side of the Pt deposit, one of the two large cracks could be seen (Figure 8c). As Ga^+ ion milling proceeded from two sides, the final TEM-lamella was extracted from the central region of the thick slice.

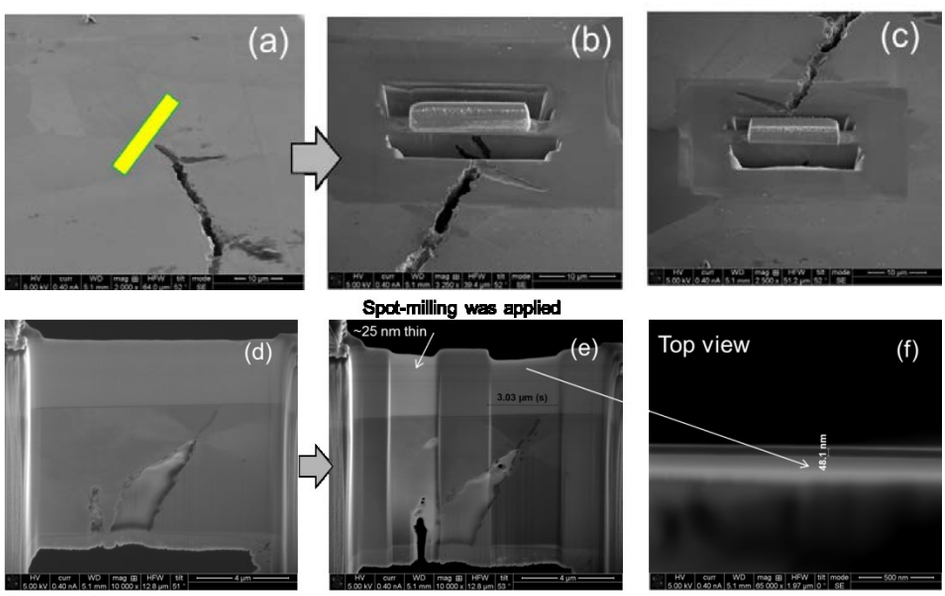

Figure 8
SEM images showing (a) the location where the TEM-lamella was prepared from, (b) and (c) the images of intermediate steps, (d) the lamella image before spot ion milling and (e and f) the image of the final TEM-lamella.

In Figure 8d two crack tips pointing at 12 and 1 o'clocks are visible. To make the two crack tip regions even thinner, spot-milling was performed. As a result, the lamella thicknesses in the regions of interest were about 25 and 48 nm, respectively (Figure 8e and f).

In Figure 9 through Figure 12, TEM images are shown for some areas of interest close to the crack tip regions. In the Me-Me grain boundaries, many chromium carbide precipitates can be seen. In Figure 10 one could see that the crack tip ended at a chromium carbide precipitate. No oxygen could be detected in the Me-Me grain boundaries close to the crack tip region. Figure 11 is a bright field TEM image showing an area close to the crack tip.

Between epoxy and metal one could detect, with Fast Fourier Transform (FFT) analysis, a zone consisting of mixed oxide and metal. As the relative orientations of the crystal planes of oxide and metal remained approximately unchanged in different locations of the FFT analysis, it is likely that the oxide was epitaxially grown on the metal surface. The oxide in this mixed zone consisted mainly of Ni and a small amount of Cr and Fe.

In Figure 12 one can see some relatively large NiO grains and some thread-like crystal in the crack tip region. Figure 13 and Figure 14 show the electron diffraction patterns and EDX spectra measured on the crystals. The electron diffraction patterns of the thread-like crystals may be matched with an orthorhombic crystal structure Ni_2FeBO_5 (a = 9.213 Å, b = 12.22 Å and c = 3.001 Å). Ni_2FeBO_5 contains 11.11 at% of B. In an EELS spectrum measured on such a thread-like crystal (Figure 15) one could see slightly elevated intensities in the range of 180 -200 eV where boron peaks would appear. An additional examination on such crystals has been reported elsewhere [20].

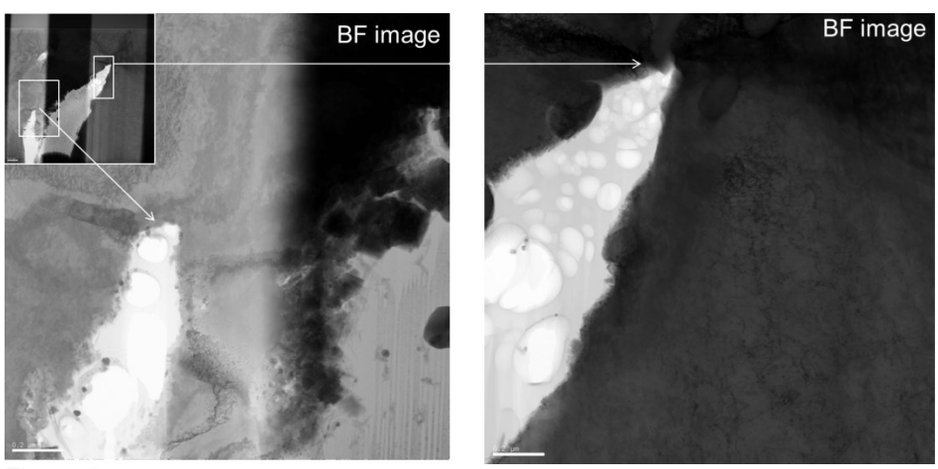

Figure 9
Bright field TEM images showing the microstructures of the regions close to the two crack tips in Figure 8.

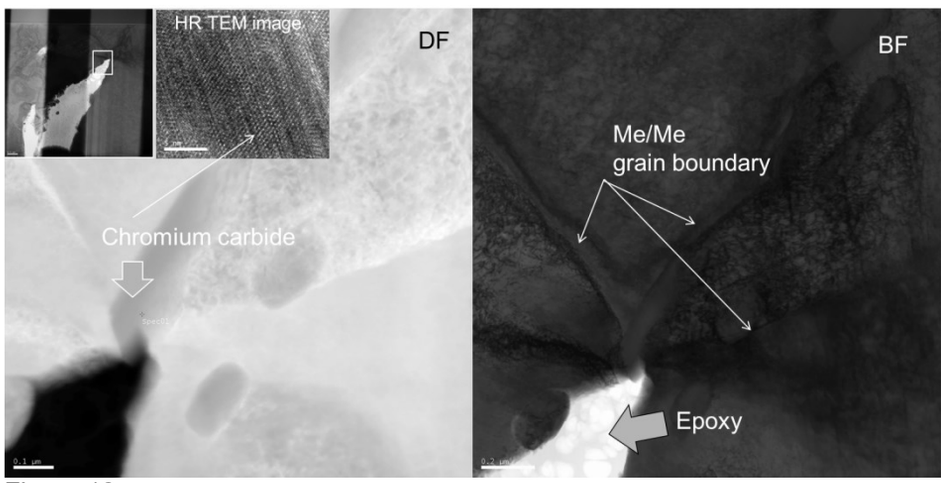

Figure 10
Dark field and bright field TEM images showing the chromium carbide in the front of the crack tip. No oxygen was detected with EDX in the metal-metal grain boundary region close to the crack tip.

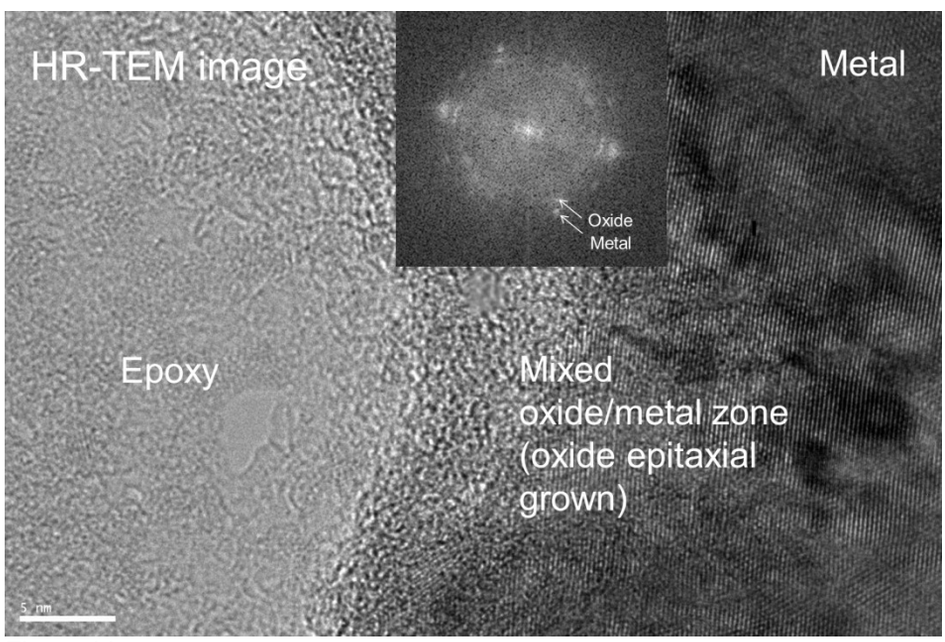

Figure 11
Bright field TEM image showing regions of epoxy, mixed oxide/metal and metal close to crack tip region. The diffraction spots from both metal and oxide appear to have similar orientations (see FFT image), suggesting possible epitaxial growth of the oxide film on the cracked metal surface.

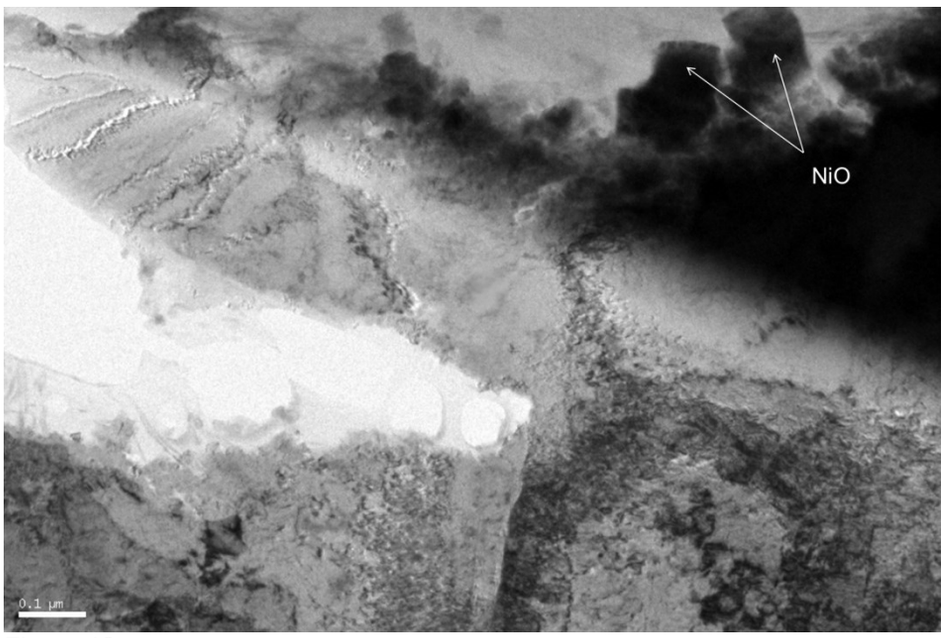

Figure 12
Bright field TEM image showing the crack tip and granular NiO grains. Some thread-like crystal on the crack surfaces are also visible.

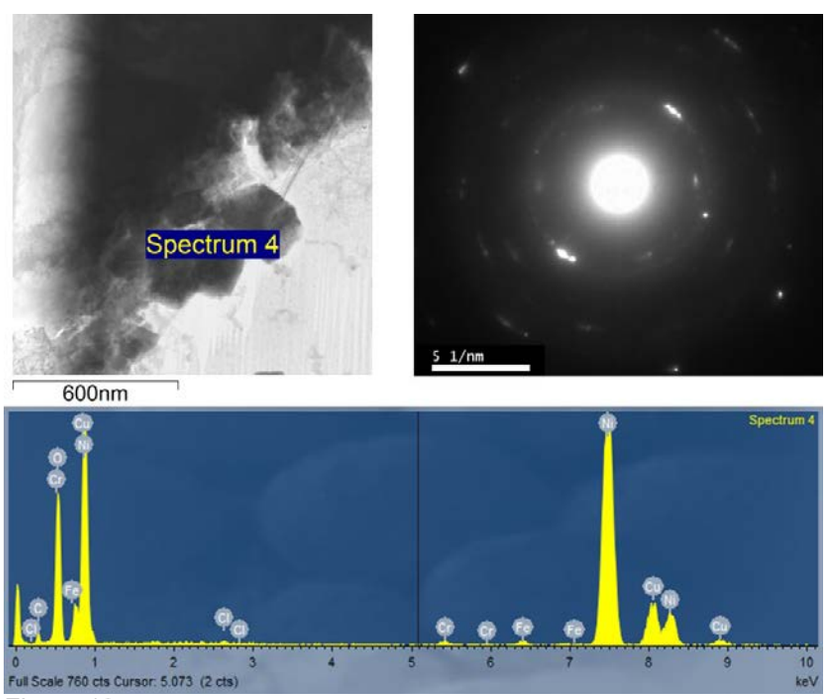

Figure 13
Electron diffraction pattern and EDX spectrum obtained for a granular NiO grain.

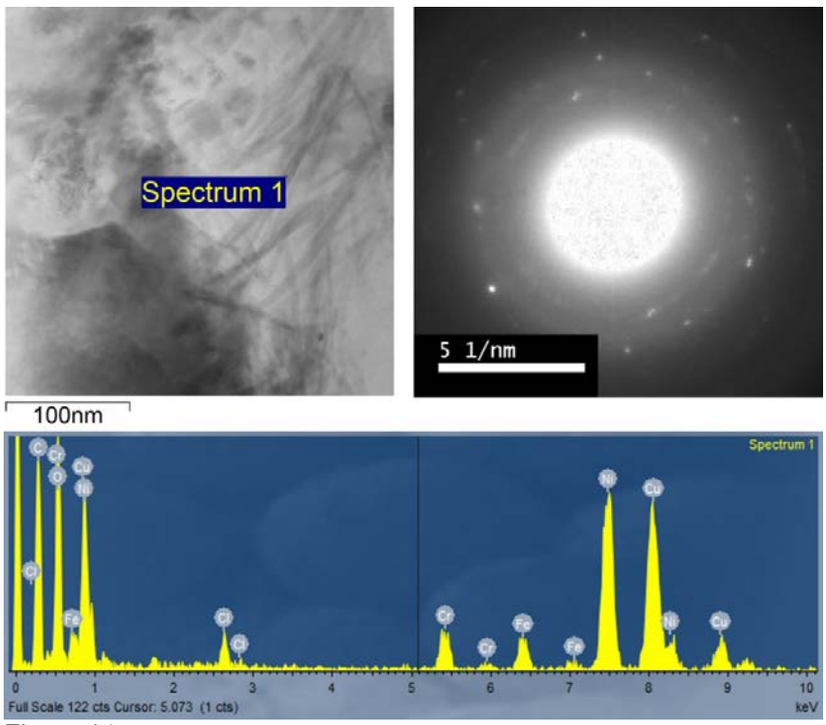

Figure 14
Electron diffraction pattern and EDX spectrum obtained for a thread-like crystal (measured elemental compositions: O 62, Cr 5, Fe 4 and Ni 29, in at%).

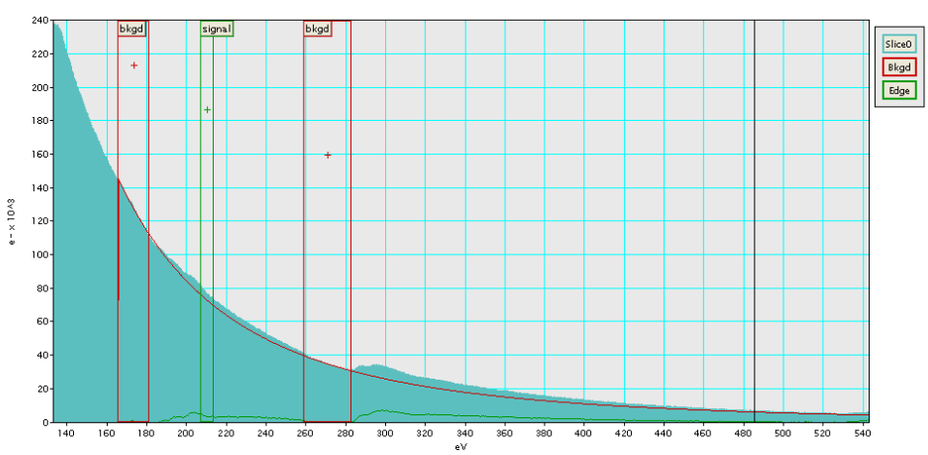

Figure 15
EELS spectrum showing peaks for Boron in the range of 180-200 eV.

3.2. Preparation of TEM-lamella no. 2

The preparation of TEM-lamella no. 2 was done following the completion of the preparation of TEM-lamella no. 1. The surface was ground and polished, with removal of approximately 24 mg metal (about 30 µm removed metal layer). The newly polished surface is shown in Figure 7. At the location where the crack tip was visible, an area was chosen for Pt deposition and

later TEM-lamella lift-out (see the green rectangle in Figure 16). With removal of material from both sides of the Pt deposit, a large crack that was hidden under the initially small crack started to appear (see Figure 17).

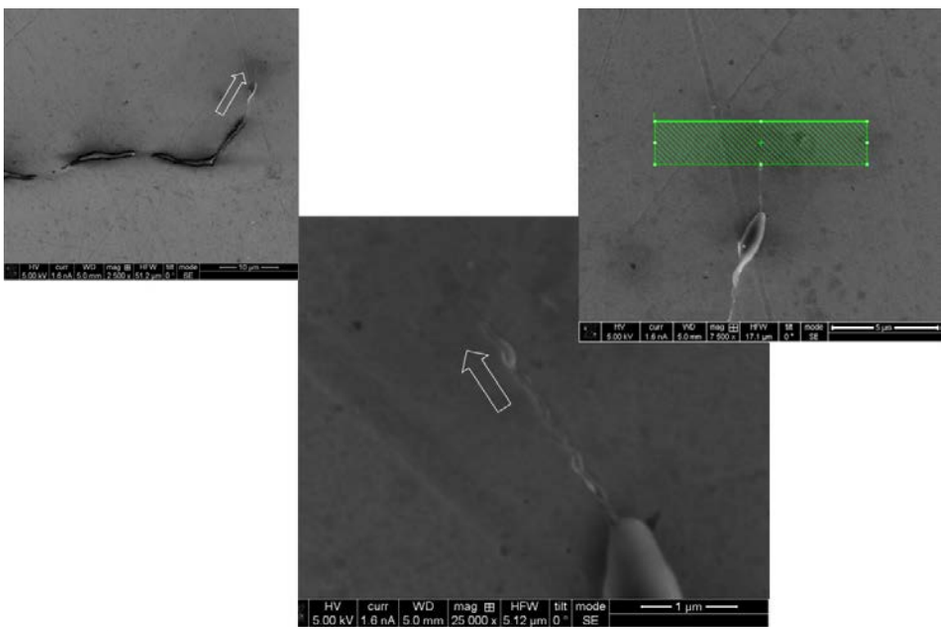

Figure 16
SEM images showing the crack tip region and the area chosen for Pt deposition and TEM lamella lift-out.

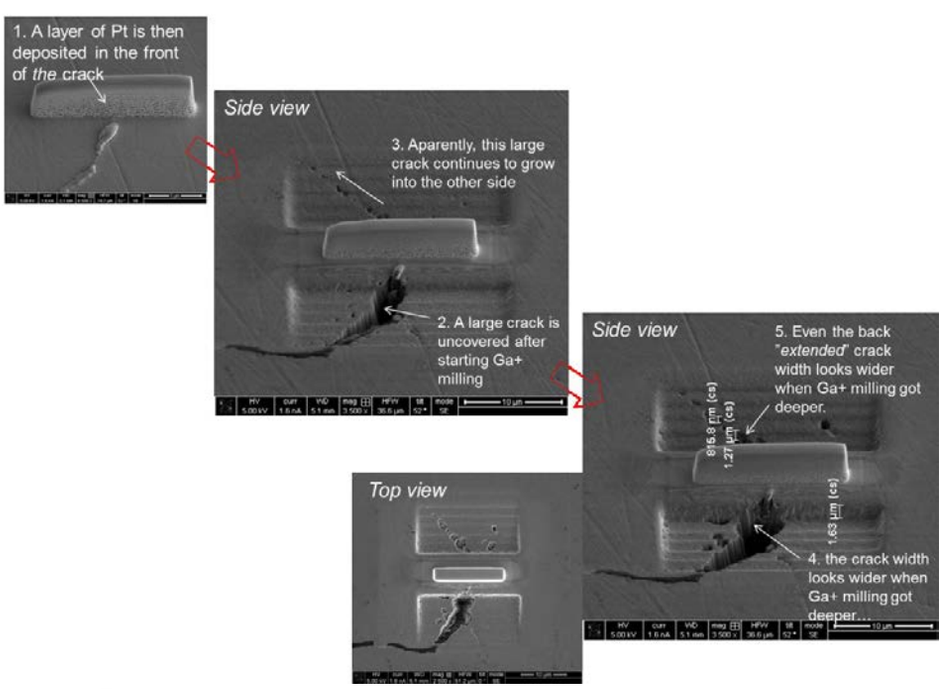

Figure 17
SEM images revealing the crack tip and its extension into the surrounding region.

With removal of metal from the crack tip area, some new crack paths in other directions were also uncovered. In the search for the crack tip, FIB was used to remove material along the newly uncovered crack paths. Two more cracks were uncovered (see Figure 18). Apparently, the new crack tip would be further away from that shown in Figure 17. An area close to the new crack tip, marked as green rectangle, was chosen for a new TEM-lamella lift-out.

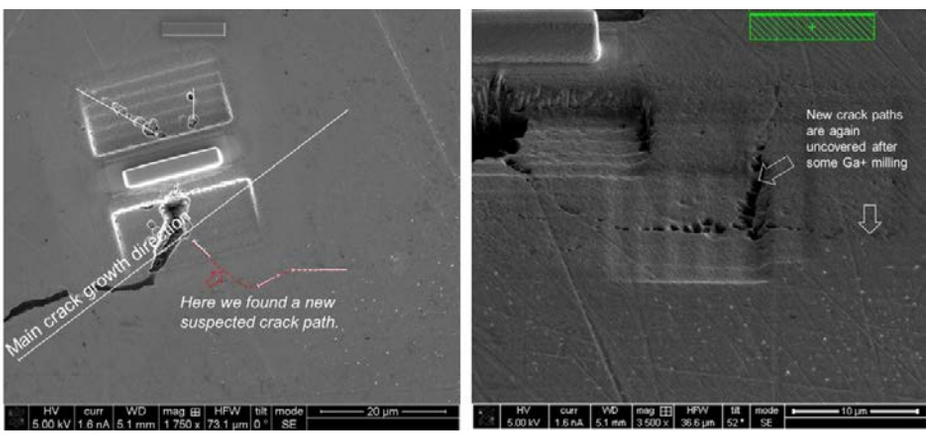

Figure 18
SEM images showing two new cracks being uncovered when a thin layer of metal was removed from the surrounding area.

With removal of metal from both sides of the Pt deposit, some large cracks under the small surface cracks were uncovered (see Figure 19). The new crack tip, appeared on the back side of the rectangular Pt cube in Figure 20, can now be easily seen. Note that this crack tip was about 30 μm further away from the crack tip initially identified in Figure 17. Since the new crack tip would be more suitable for the purpose of this work, a new area just ahead of the new crack tip, the green rectangle in Figure 20, was chosen for new TEM-lamella lift-out. With removal of metal from the area close to the Pt deposit, some large cracks were uncovered initially but disappeared when Ga^+ ion milling approached the Pt deposit from the side.

Figure 21 shows a TEM bright field image of a part of the TEM-lamella prepared. The top part of the lamella was about 50 nm or thinner in thickness. At the top region of the lamella one can see a layer of recrystallized metal. This was likely a result of the Ga^+ milling in this area during the crack tip hunting before Pt was deposited. In this lamella, one can see Me-Me grain boundaries in which there were a number of chromium carbide precipitates. An EELS measurement showed an atomic ratio of Cr to C of ~2, suggesting that the carbide was Cr_7C_3 (orthorhombic, a = 7.014 Å, b = 12.15 and c = 4.532 Å). Figure 22 through Figure 24 show some TEM bright field images of some locations of the TEM lamella. Figure 25 is a high resolution TEM image of a chromium carbide precipitate.

EDX measurements were performed at various locations in the Me-Me grain boundaries in this lamella and no oxygen as oxides could be detected.

Apparently, the crack did not pass through the region from which this TEM-lamella was prepared. In other words, this lamella did not contain any crack tip but it may be very close to the crack tip region.

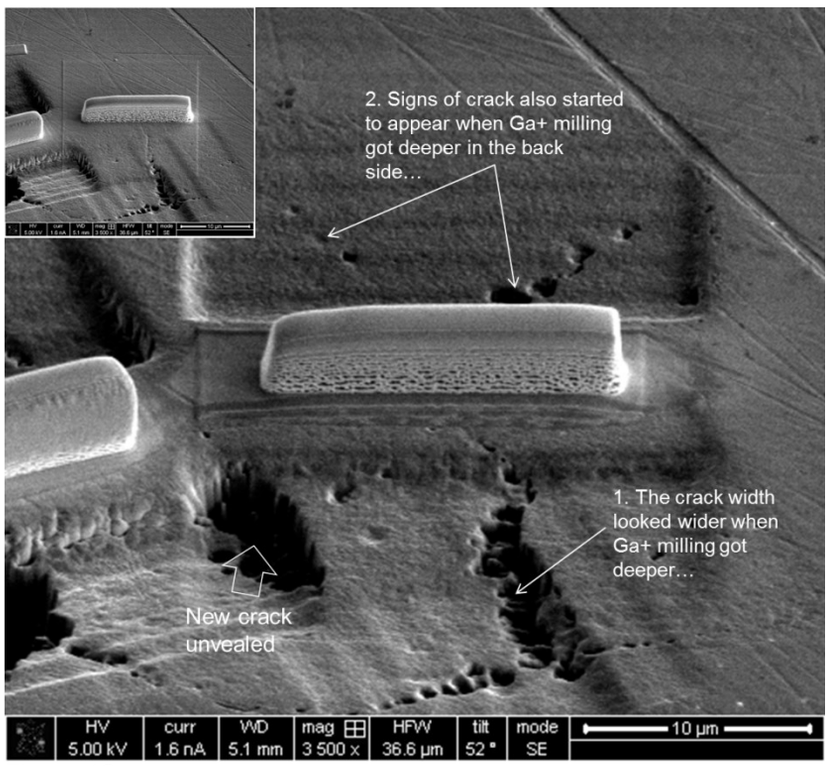

Figure 19
SEM images showing new cracks being uncovered in the region close to the Pt deposit.

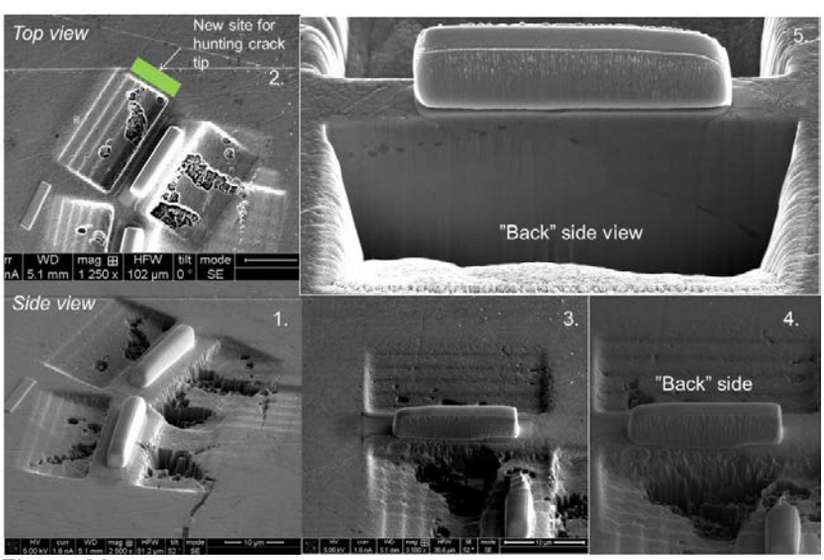

Figure 20
SEM images showing the new crack tip and some uncovered large cracks close to the Pt deposit.

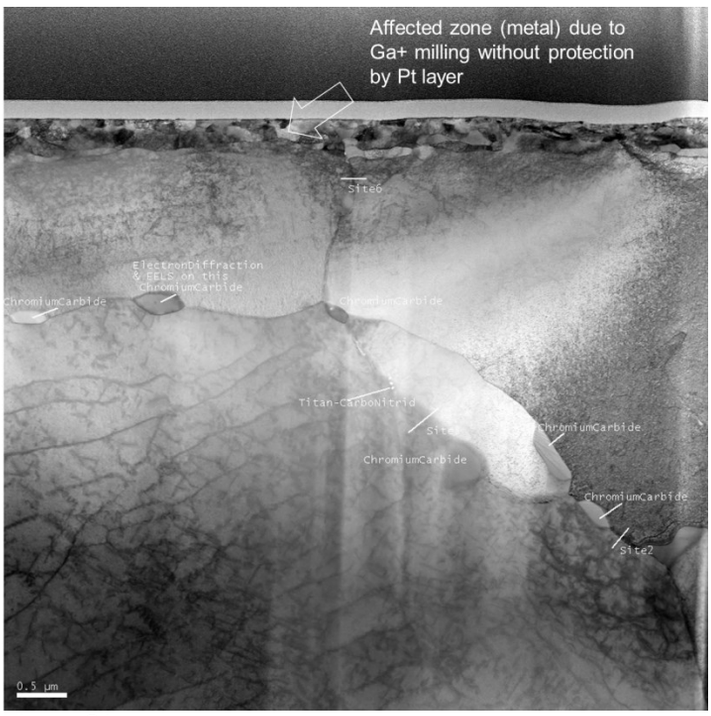

Figure 21
TEM bright field image showing a part of TEM-lamella close to the crack tip region.

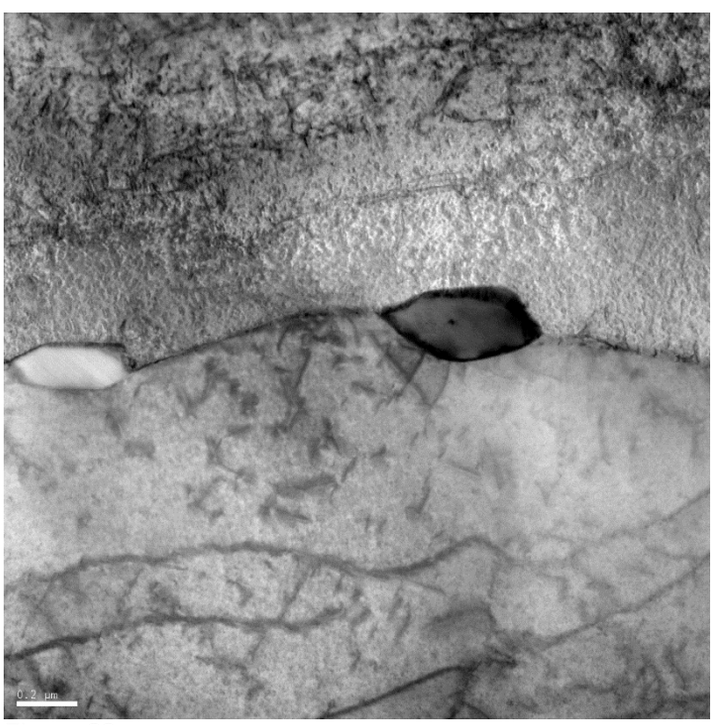

Figure 22
TEM bright field image of an area including precipitates in the grain boundary.

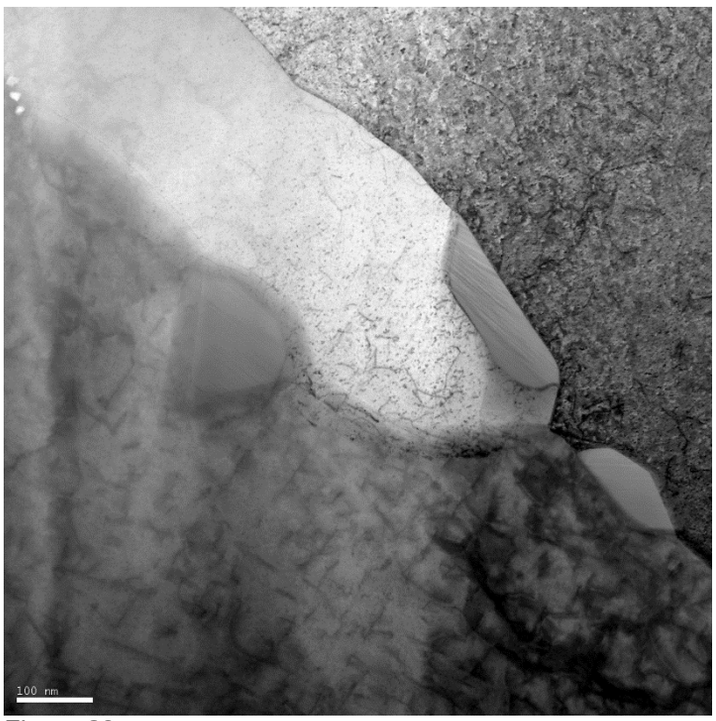

Figure 23
TEM bright field image of an area including precipitates in the grain boundaries.

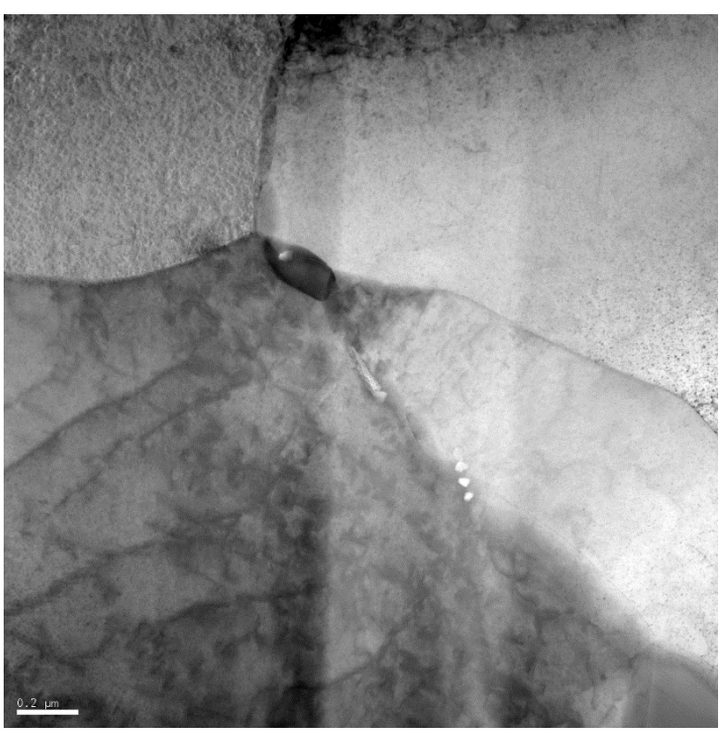

Figure 24
TEM bright field image of an area including precipitates in the grain boundaries.

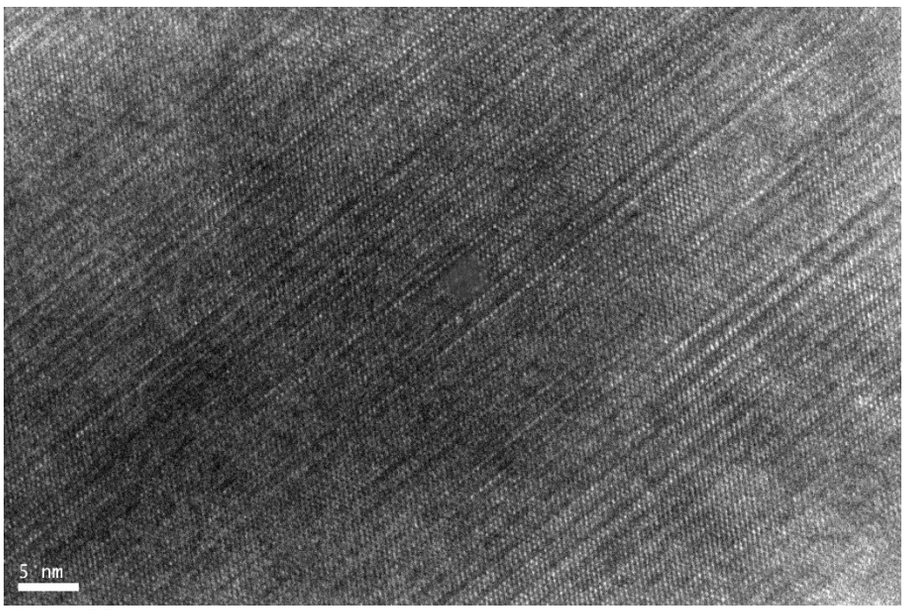

Figure 25
High resolution TEM image of chromium carbide precipitate.

4. Discussion

In this work, two TEM lamellas were prepared from two crack tip regions. The preparation of the first lamella was relatively straightforward. The TEM-lamella was extremely thin and of high quality. Examination of the oxide film in the crack tip region was proved to be possible. The second TEM-lamella preparation was, however, not so straight forward and led to some interesting observations regarding the crack path. The crack tips were found to extend a few micrometers beyond the crack tip location initially identified. The second TEM-lamella prepared did not contain any crack tips or oxides but it was indeed from a location very close to the crack tip.

The method as described in this report has demonstrated the ease of use in preparation of high quality TEM-lamellas from a crack tip in a standard compact tension specimen. Basically, the method is applicable to similar specimens which contain cracks.

Based on the limited scope of the TEM examination performed on the prepared lamellas, one has obtained the following new observations about crack tips and the surrounding oxides:

Crack tips are indeed 3 dimensional in a crack front. On a polished surface where the crack front is revealed in the way as presented, there may be many crack tips which extend in different lengths into metal grain boundaries of different directions. In other words, in a crack front there may be many crack tips which are far apart from each other. In fact, such an uneven crack front can be readily seen in a metallographic examination. Along the main crack path the distance from a crack tip to an adjacent one could be up to a 20 to 30 micrometers or more, depending on the metal grain sizes at the crack front.

The finding of epoxy material in the supposedly very narrow region of the crack tip suggests that the water chemistry environment in the narrow crack tip region may, after all, not be very different from that in bulk reactor water. As viscosity of high temperature and high pressure water must be much smaller than the epoxy used it must have been relatively easy for the water and other chemical species to permeate into the numerous large micro-size voids in the crack paths or close to the crack tips. According to Jenssen [19], the cracks in the samples examined were much wider than expected for intergranular SCC. It is possible water and even less so epoxy would have had difficulties reaching the tip had the crack been much narrower. His explanation may be that the part of the crack front examined in this study arrested during SCC testing. The wide crack indicates that it may not have been actively growing SCC, and perhaps the relatively wide crack may have been a result of crack blunting.

The result of the preliminary TEM examination on the oxide films in the crack tip region (TEM lamella no. 1) is in agreement with that reported previously using TEM-lamella lift-out from a cracked surface after the metallography examination [6]. This has confirmed the usefulness and adequateness of the present method.

5. Conclusions

Based on the examinations performed in this work, one may conclude the following:

(1) The method as demonstrated in this work can be applied for preparation of high quality TEM-lamellas from crack tip regions. The method is easy to use and the sample can be re-used after each TEM-lamella lift-out through usual mechanical grinding and polishing.
(2) The three dimensional crack tips in a crack front imply that one should easily find multiple crack tips in the surroundings of a crack tip initially spotted on a polished surface.

Acknowledgements

Professor Lyubov Belova and Dr. Anastasia Riazanova (Royal Institute of Technology, Sweden) performed TEM-lamella preparation with FIB/SEM. Dr. Fredrik Lindberg (Swerea KIMAB AB) made TEM examinations on the prepared TEM-lamellas. Mr. Anders Jenssen, Mr. Johan Stjärnsäter and Dr. Pia Tejland (Studsvik) contributed with invaluable ideas through scientific discussions in the course of this work. Mr. Daniel Lyth assisted with sample cutting with electric discharge machining. Mr. Peter Ekström (Swedish Radiation Safety Authority) is gratefully acknowledged for his insightful encouragement which has made this work possible. This work is financially supported by Swedish Radiation Safety Authority.

References

[1] König, M and Norring, K. (2002). *Influence of hydrogen on the crack growth rate of Alloy 600 in simulated primary side PWR environment.* Studsvik Nuclear AB, Sweden. (STUDSVIK/N(K)-02/025).

[2] König, M. (2006). *The Influence of Hydrogen on the Crack Growth Rate of Alloy 600 in Simulated Primary Water at 330ºC.* Studsvik Nuclear AB, Sweden. (STUDSVIK/N-06/055).

[3] Norring, K. (2010). Studsvik Nuclear AB, Sweden (STUDSVIK/N-10/014).

[4] Molander, A., Norring, K., Andersson, P-O and Efsing, P. (2012). *Effects of water chemistry on PWSCC initiation and propagation in Alloy 600.* Presented at Eurocorr in Stockholm 2012.

[5] Molander, A., Norring, K., Andersson, P-O and Efsing, P. (2011). *Effects of water chemistry on PWSCC initiation and propagation in Alloy 600.* 15th Internat Symp on Environmental Degradation of Materials in Nuclear Power Systems - Water Reactors. TMS, 2011.

[6] Stjärnsäter, J. and Chen, J.(2013) *The effect of hydrogen on the oxide formation and crack growth rate in Alloy 600 of CT specimens exposed in simulated PWR environments*. Studsvik Nuclear AB, Sweden. (STUDSVIK/N-13/158).

[7] Cassagne, T. et. al. (1997). *An update on the influence of hydrogen on the PWSCC of nickel base alloys in high temperature water*. 8th Internat Symp on Environmental Degradation of Materials in Nuclear Power Systems, Proc. ANS, p. 307-315.

[8] Morton, D., Attanasio, S., Richey, E and Young, G. (2005). *In Search of the True Temperature and Stress Intensity Factor Dependencies for PWSCC.* 12th Internat Symp on Environmental Degradation of Materials in Nuclear Power Systems - Water Reactors. TMS, 2005.

[9] Andresen, P., Reid, R. and Wilson, J. (2009). *SCC Mitigation of Ni Alloys and Weld Metals by Optimizing Dissolved H_2.* 14th Internat Symp on Environmental Degradation of Materials in Nuclear Power Systems, Virginia Beach, VA, August 2009.

[10] Dozaki, K., Akutagawa, D., Nagata, N., Takiguchi, H and Norring, K. (2010) *Effect of Hydrogen content in PWR Primary Water on PWSCC Initiation Property*. Journal of Advanced Maintanance, Vol. 2, 65-76. Japan Society Maintenology.

[11] Marks, C., Dumouchel, M., Reid, R. and White, G. (2011). *Quantifying the Benefit of Chemical Mitigation of PWSCC via Zink Addition or Hydrogen Optimization.* 15th Internat Symp on Environmental Degradation of Materials in Nuclear Power Systems - Water Reactors. TMS, 2011.

[12] Combrade, P. et al. (2005). *Oxidation of Ni Base Alloys in PWR Water: Oxide Layer and Associated Damage to the Base Metal.* 12th Internat Symp on Environmental Degradation of Materials in Nuclear Power Systems, Warrendale, PA, August 2005.

[13] R. W. Staehle, (2008). *The small dimensions of stress corrosion cracking-tight cracks*. International Conference on Water Chemistry of Nuclear Reactor Systems, October 23-26, 2006, Jeju lsland, KOREA.

[14] L. E. Thomas and S. M. Bruemmer, (1999). *Insights into environmental degradation mechanisms from analytical transmission electron microscopy of SCC cracks*. 9th Inter Symposium on Environmental Degradation of Materials in Nuclear Power Systems – Water Reactors – Edited by F.P Ford, S.M. Bruemmer, and G.S. Was, The Minerals, Metals & Materials Society (TMS), 1999.

[15] Lim, Y. S., Kim, H. P., and Hwang, S. S. (2013). *Microstructural characterization on intergranular stress corrosion cracking of Alloy 600 in PWR primary water environment.* J. Nuclear Materials. 440, 46-54..

[16] Sundberg, J., Jenssen, A. (2004). *Round Robin-provning av nickelbaslegeringarna Alloy 600 och Alloy 182 för jämförelse och optimering av spricktillväxtdata.* Studsvik Nuclear AB, Sverige. (STUDSVIK/N-04/119).

[17] Stjärnsäter, J. (2006). *Spricktillväxt i Alloy 600 i simulerad BWR-miljö.* Studsvik Nuclear AB, Sverige. (STUDSVIK/N-06/164).

[18] Stjärnsäter, J. (2012). *Inverkan av temperaturen på spricktillväxthastigheten i sensibiliserat rostfritt stål av typ 304 i NWC-miljö med sulfat.* Studsvik Nuclear AB, Sverige. (STUDSVIK/N-12/029).

[19] Jensen, A. Private communication (2013).

[20] Chen, J., Lindberg, F., Wells, D. and Bengtsson, B. (2014). *EELS and Electron Diffraction Studies on Possible Bonaccordite Crystals in PWR Fuel CRUD and in Oxide Films of Alloy 600 Material.* Paper ID. 10149. In the proceedings of NPC 2014, Sapporo, Japan.

Appendix A

Properties Alloy 600 (Material 196)
Produced by: Metals Technology Inc.
Heat Number: 22474 (produced 1999)
Heat treatment: Mill annealed

Chemical analysis
(by wt-%)

	Ladle-analysis	Check-analysis
C	0.04	0.037
Si	0.18	0.22
Mn	0.24	0.24
P	0.010	0.012
S	0.002	0.001
Cr	15.25	15.9
Ni	75.94	74.3
Co	0.18	0.34
Ti	0.28	0.30
Al	0.22	0.15
Cu	0.09	0.05
Fe	7.34	8.4

Mechanical properties at temperature

	r. t.	300 °C
Rp0.2 MPa	311	270
Rm MPa	674	625
A_5 %	40	40
Z %	64	58

Microhardness
HV 169

Grain size
38 µm
ASTM: 6-7

Stress-strain curves
Room temperature

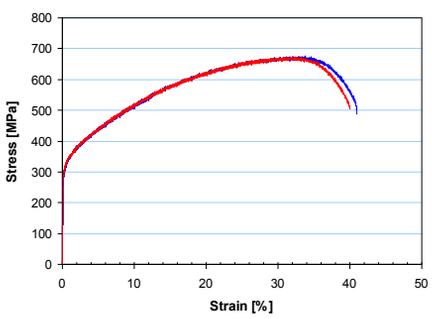

300 °C

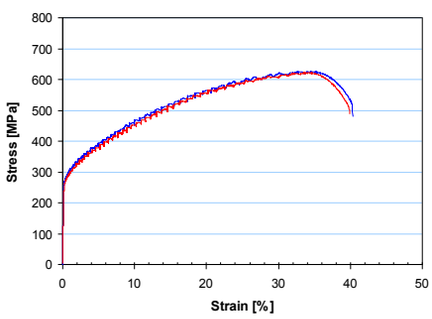

Microstructure

Images from light optical microscopy

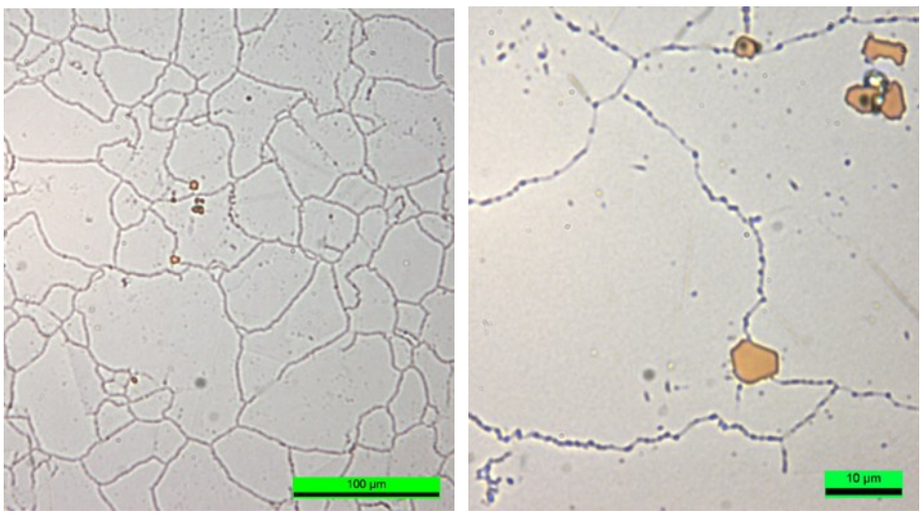

Images from scanning electron microscopy

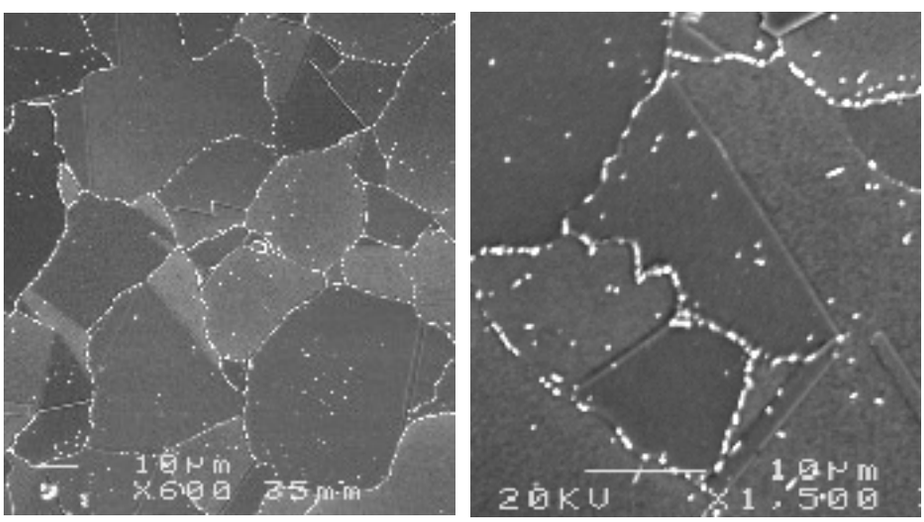

2015:07

The Swedish Radiation Safety Authority has a comprehensive responsibility to ensure that society is safe from the effects of radiation. The Authority works to achieve radiation safety in a number of areas: nuclear power, medical care as well as commercial products and services. The Authority also works to achieve protection from natural radiation and to increase the level of radiation safety internationally.

The Swedish Radiation Safety Authority works proactively and preventively to protect people and the environment from the harmful effects of radiation, now and in the future. The Authority issues regulations and supervises compliance, while also supporting research, providing training and information, and issuing advice. Often, activities involving radiation require licences issued by the Authority. The Swedish Radiation Safety Authority maintains emergency preparedness around the clock with the aim of limiting the aftermath of radiation accidents and the unintentional spreading of radioactive substances. The Authority participates in international co-operation in order to promote radiation safety and finances projects aiming to raise the level of radiation safety in certain Eastern European countries.

The Authority reports to the Ministry of the Environment and has around 315 employees with competencies in the fields of engineering, natural and behavioural sciences, law, economics and communications. We have received quality, environmental and working environment certification.

Strålsäkerhetsmyndigheten
Swedish Radiation Safety Authority

SE-171 16 Stockholm
Solna strandväg 96

Tel: +46 8 799 40 00
Fax: +46 8 799 40 10

E-mail: registrator@ssm.se
Web: stralsakerhetsmyndigheten.se